Journal of Fiber Bioengineering and Informatics 7:1 (2014) 13–22
doi:10.3993/jfbi03201402

Study on the Bending Fatigue Behavior of Single Aramid Fibers by a Novel Bending Fatigue Test Method

Guangming Cai [a,*], Wenfang Song [b], Xin Cui [c], Weidong Yu [a,c]

[a] *College of Textile, Wuhan Textile University, Wuhan 430073, China*

[b] *Department of Building and Real Estate, The Hong Kong Polytechnic University, Hung Hom Kowloon, Hong Kong, China*

[c] *College of Textile, Donghua University, Shanghai 201620, China*

Abstract

In this paper, we report a bending fatigue testing apparatus which can test the bending fatigue resistance of single Kevlar 49 fiber by setting the pretension and bending angle. The cyclic tension and the (number of cyclic bending of fiber) were recorded by this apparatus. The cyclic tension curve showed that the tension changes in periods during the bending fatigue process. The cyclic tension was theoretically analyzed and found that the bending angle had significant effect on the cyclic tension. The cyclic bending number N of Kevlar 49 fiber was plotted as a function of pretension S using S-N curves, which shows that the bending angle and pretension have a significant effect on the fatigue lifetime of a fiber. The bending fatigue morphologies of Kevlar 49 fiber explained the bending failure mechanism of the Kevlar 49 fibers.

Keywords: Test Method; Bending Fatigue; Kevlar 49 Fiber; Cyclic Tension; Fracture Morphology

1 Introduction

As we all know, aramid fibers have applied wide range of application in our day to day life. Kevlar fiber as a kind of aramid fibers, has an extensive application in aerospace, militant affairs and thermal protective materials in recent years. Although the aramid fibers have good tension strength, the compressive strength and shearing of aramid fibers are poor. The poor bending and shearing strength restrict their applications in many aspects [1]. An important method to evaluate the compressive strength of fiber is bending test, because the major fracture is caused by compressive and shearing force. There are many previous researchers who studied tensile fatigue of single fiber under different pretension [2-5], however, studies on bending fatigue are scarce. Hearle studied the flexural fatigue of Kevlar 29 fiber [6]. Liu XY studied the bending fatigue properties of single aramid fiber at different pretensions [7]. Burgoynet investigated the bending fatigue of aramid ropes [8] and Kazuto studied the effect of wet on the bending fatigue properties of single

*Corresponding author.
Email address: guangmingcai2006@163.com (Guangming Cai).

aramid fiber [9]. Kohji Minoshima discussed the bending fatigue behavior of single aramid fiber in vacuum and air environment and found that the aramid fiber has a better fatigue resistance in vacuum [10]. Cai used the sample bending fatigue apparatus studied the bending fatigue of some high performance fibers [11-12]. Overall, reporters characterize the bending fatigue of aramid fibers using different testing apparatus to provide the evaluation methods for bending fatigue of fibers. However, these studies only discussed the effect of pretension on fatigue life and had no report on the effect of bending angle on fatigue life. Also these devices can only record the number of bending fatigue, not observe fiber bending fatigue failure process of fiber and record the cyclic tension under fatigue process. When the pretension is the same, the amplitude of cyclic tension is larger at a large bending angle. So we need discuss the effect of bending angle on the fatigue life. At the same time, we can analyze the bending failure mechanism by observe fiber bending fatigue failure process of fiber..

This paper will study the bending fatigue properties of Kevlar49 fiber using a new testing apparatus which is developed by authors [13]. The bending fatigue behavior of single Kevlar49 fiber was measured and the effects of pretension, the bending angle on fatigue life of Kevlar49 fiber were discussed. The bending fatigue fracture ends of the Kevlar49 fiber were observed using an optical microscope, which can explain the fracture mechanism of Kevlar 49 fibers.

2 Experimental

2.1 Testing Apparatus

Fig. 1 (a) shows the principle of test apparatus and Fig. 1 (b) is test apparatus. The bending fatigue test system is comprised of eight parts: 1) The upper jaw, 2) The positioning pin, 3) The lower jaw, 4) The running plane, 5) The optical microscope, 6) The CCD camera, 7) The temperature sensor, and 8) The heater. The jaws are used to clamp the fiber. The positioning pin

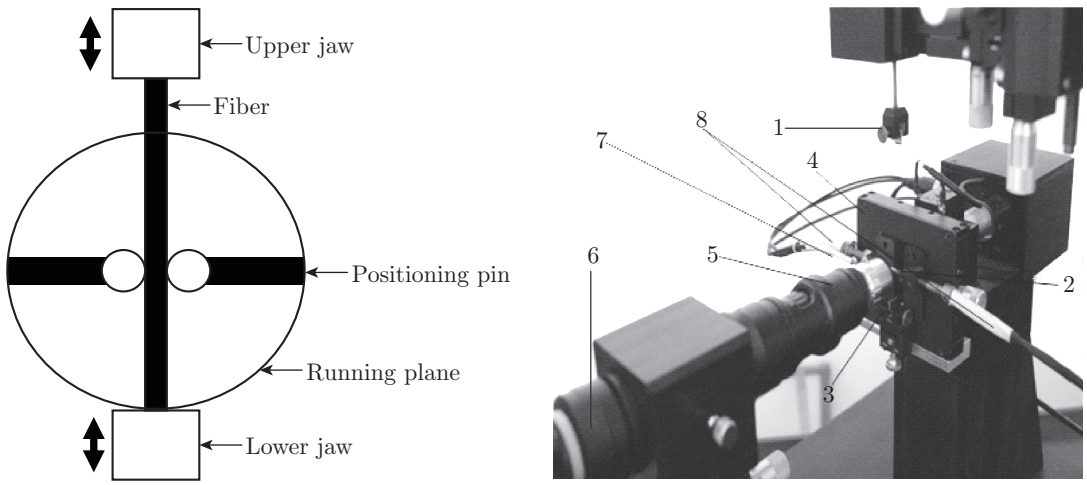

1 — Upper jaw; 2 — Positioning pin; 3 — Lower jaw; 4 — Running plane; 5 — Optical microscope; 6 — CCD camera; 7 — Temperature sensor; 8 — Heater

Fig. 1: The real photo of bending fatigue test apparatus (a) is the principle of test, (b) is test apparatus

can handhold the fiber and fix the bending point under bending fatigue. The fiber is bent when the running plane rotates at different angles. The optical microscope and CCD camera are used to observe the bending fatigue fracture morphology of the fiber. The heater and temperature sensor are used to control the temperature of bending point. The temperature can be regulated electrically from room temperature up to 200 °C.

Figs. 2 and 3 show the details of the apparatus, the jaw is used to fix test specimen which is used to clamp different materials such as fiber. The positioning pin can clamp the fiber and make the fiber (fixed-point bending). Compared with the previous apparatus, this testing apparatus has the following characteristics:

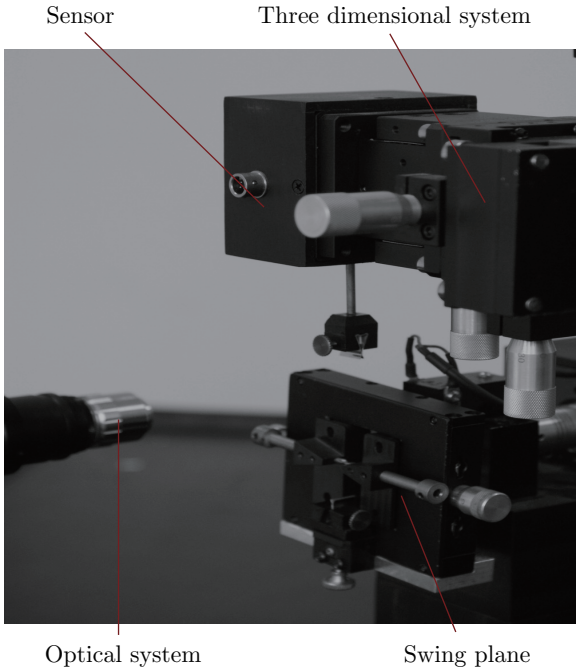

Fig. 2: The digital bending fatigue test system

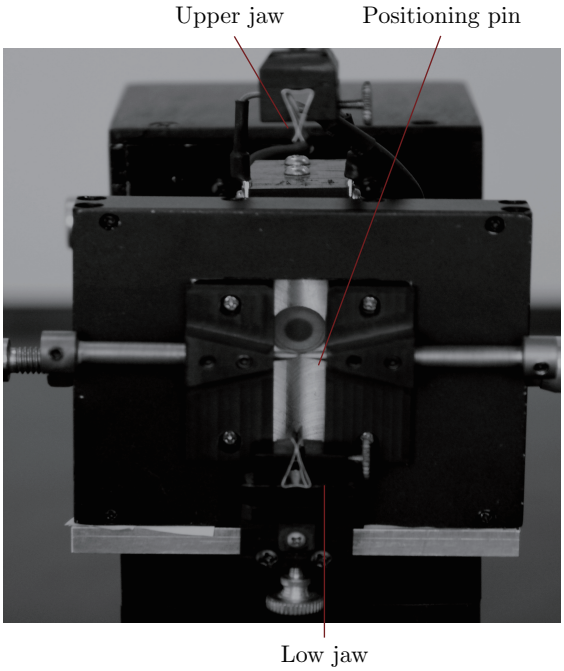

Fig. 3: The details of the bending fatigue test system

(1) Fixed-point bending

(2) Recording cyclic tension value of materials under bending process

(3) With optical system, monitoring the swing process of materials, fixing the position of materials and screening the rupture morphology of fibers

(4) Setting parameters conveniently: pre-tension, bending angle

2.2 Experimental Materials and Procedure

The single Kevlar 49 fiber was tested in this bending fatigue experiment. The linear density of single Kevlar 49 was 2.2 dtex. The gauge length adopted for the bending fatigue tests was 60 mm. The pretension and the bending angles were set before the experiment. The number of the cyclic bending and cyclic tension were obtained, the fracture ends were also screened in this experiment. The test numbers of every specimen are set as 10 times and all the measurements were conducted under 25 °C and 65% relative humidity.

3 Results and Discussion

3.1 Theoretical Analyses of Cyclic Tension under Bending Process

Equation (1) is the function of the stress σ versus the strain ε. Fig. 4 is the curve of σ versus ε of Kevlar 49 fiber. It can be found that there is a linear relationship between stress σ and strain ε. The elongation of fiber changes when the fiber cyclic bends, then the cyclic stress will change.

$$\sigma = E\varepsilon \tag{1}$$

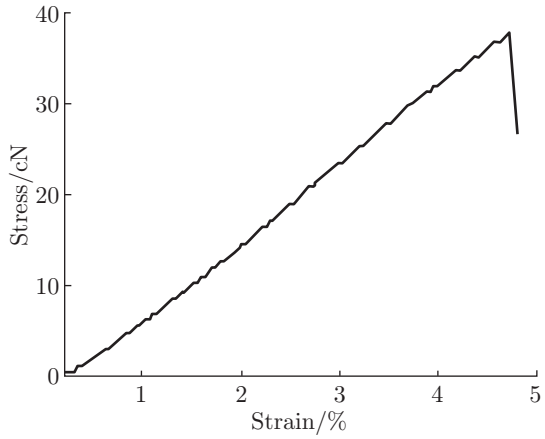

Fig. 4: The curves of σ versus ε of Kevlar 49 fiber

It is found that an additional fiber elongation resulted from the diameter of a positioning pin when the fiber bends, as shown in Fig. 5 (a). Fig. 5 (b) is the mechanical model of fiber during bending process. It can be seen from Fig. 5 (b) that the AM region of fiber is only in tension and the MO region is in tension and bending. The contact load in MO region includes tangential load σ and normal load N. The tangential load σ can be obtained by calculating the additional fiber elongation.

Fiber AB is loaded under the pre-tension σ_0 and the length of AO is l, the round O_1 is the positioning pin and its radius is r. When the fiber bends, the fixed point O is immovable. When the positioning pin rotates at an angle θ, the positioning pin rotates around O_2 and the fiber changes to AMOB. According to Fig. 5 (a), the line AM is tangential to the positioning pin and the point of intersection of the line AO and round O_2 is E and the line O_2N Perpendicular to AO, so the excess fiber length can be calculated by geometric modeling. Based on the geometric theorem, the length AM is

$$AM = \sqrt{AO * AE} \tag{2}$$

According to the geometric relationship, we can obtain:

$$ON = OO_2 \sin\theta = r\sin\theta \quad O_2N = r\cos\theta \quad AE = AO - OE = l - 2r\sin\theta,$$

Equation (2) can be written as:

$$AM = \sqrt{l^2 - 2lr\sin\theta} \tag{3}$$

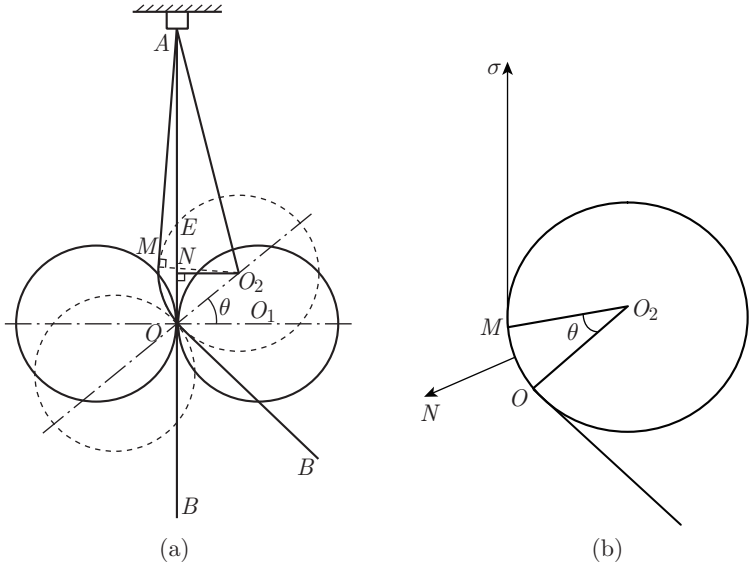

Fig. 5: The fundamental structure of fiber bending process. (a) The schematic structure of fiber bending process, (b) The mechanical model of fiber during bending process

We can get

$$AO_2 = \sqrt{l^2 + r^2 - 2lr\sin\theta} \tag{4}$$

It is easy to obtain:

$$\angle MO_2O = \theta + \angle MO_2N; \quad \angle MO_1N = \angle AO_2N - \angle AO_2M \tag{5}$$
$$\cos(\angle AO_2N) = \frac{O_2N}{AO_2}, \quad \cos(\angle AO_2M) = \frac{O_2M}{AO_2}$$

Hence we know:

$$\angle AO_2N = \arccos\frac{r\cos\theta}{\sqrt{l^2 + r^2 - 2lr\sin\theta}} \tag{6}$$

$$\angle AO_2M = \arccos\frac{r}{\sqrt{l^2 + r^2 - 2lr\sin\theta}} \tag{7}$$

The length of the arc MO is obtained:

$$MO = r\Big(\theta + \arccos\frac{r\cos\theta}{\sqrt{l^2 + r^2 - 2lr\sin\theta}} - \arccos\frac{r}{\sqrt{l^2 + r^2 - 2lr\sin\theta}}\Big) \tag{8}$$

So we can calculate the length l_1 of fiber after bending at an angle θ:

$$l_1 = \sqrt{l^2 - 2lr\sin\theta} + r\Big(\theta + \arccos\frac{r\cos\theta}{\sqrt{l^2 + r^2 - 2lr\sin\theta}} - \arccos\frac{r}{\sqrt{l^2 + r^2 - 2lr\sin\theta}}\Big) \tag{9}$$

Assuming that the elastic modulus of the fiber is constant, the cyclic stress can be obtained:

$$\sigma = E\frac{\sqrt{l^2 - 2lr\sin\theta} + r\Big(\theta + \arccos\frac{r\cos\theta}{\sqrt{l^2 + r^2 - 2lr\sin\theta}} - \arccos\frac{r}{\sqrt{l^2 + r^2 - 2lr\sin\theta}}\Big) - l}{l} + \sigma_0 \tag{10}$$

where E is the elastic modulus of fiber, r is the radius of positioning pin and l is the length of fiber before circumrotating.

Based on equation (10), the cyclic stress is influenced by the following parameters: the pretension σ_0; (2) the radius of positioning pin; (3) the circumrotation angle θ. Assuming that the circumrotation angles are up to 60° and 75°, the periods of circumrotation is 2 seconds, the radius of the positioning pin is 0.2 mm, the length l of fiber is 40 mm and its elastic modulus is 780 cN/dtex , the cyclic stress can be calculated from equation (10). The numerical analysis results (Fig. 6) show that the cyclic stress increased with the increasing circumrotation angle. This is due to the fact that the additional fiber elongation is increased when increasing the circumrotation angle.

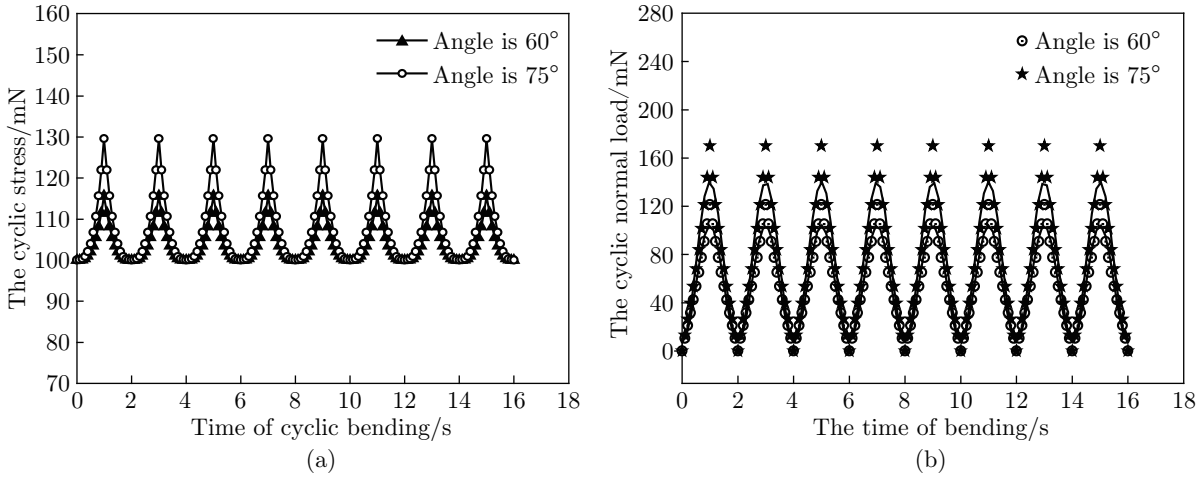

Fig. 6: The theoretical curves of cyclic tension (The circumrotate angle are 60° and 75° respectively) (a) The cyclic tangential load (b) The cyclic normal load

It assumes that the surface of positioning pin is smooth and has no friction. So the normal load N can be obtained by the equation (11)

$$N = \sigma \cdot \left(\theta + \arccos \frac{r \cos \theta}{\sqrt{l^2 + r^2 - 2lr \sin \theta}} - \arccos \frac{r}{\sqrt{l^2 + r^2 - 2lr \sin \theta}} \right) \tag{11}$$

The numerical analysis results (Fig. 6) shows that the normal load N increased with the increasing circumrotation angle. It can be found that the MO region of the fiber was suffered from both repeated tangential load σ and normal load N while the AM region of the fiber was suffered only from tangential load σ. So the position of the fiber surface rupture is MO region.

3.2 Cyclic Tension Curve of Kevlar 49 Fiber

The cyclic tension of Kevlar 49 fiber during bending process repeatedly (the pretension is 100 mN and the circumrotation angle is 60°) was shown in Fig. 7 (a). The fiber elongation resulted from the diameter of a positioning pin when the fiber bends, which led to stress fluctuation. It can be found that the cyclic stress changes in periods. The number of cyclic bend N can be acquired by the period T of cyclic curve and the fatigue fracture time t. Fig. 7 (b) shows the effect of circumrotation angles on the amplitude of the cyclic stress, from which it can be found that the amplitude is larger at a large circumrotation angle.

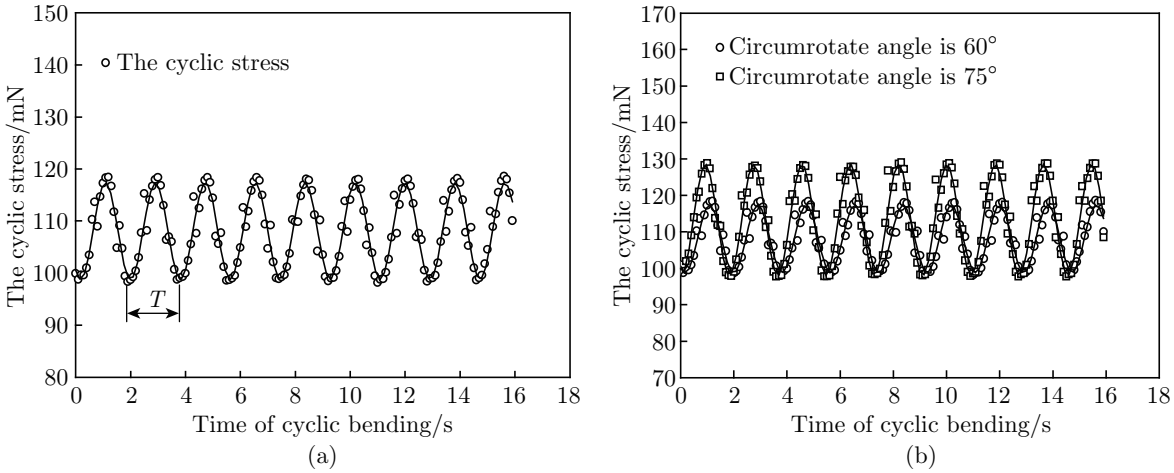

Fig. 7: (a) The cyclic stress of single Kevlar 49 fiber; (b) The cyclic stress under different circumrotation angles

3.3 Effect of Pre-tension on Bending Fatigue Lifetime

Effect of factors affecting the bending fatigue life of fiber materials includes pretension, bending angle and bending frequency. Many reports had discussed the fatigue of a polymer. These investigations had for their basis Zhurov's kinetic concept of the mechanical deterioration of polymers defined by the general equation

$$\tau = \tau_0 \exp[(U_0 - \alpha\sigma)/\mathrm{KT}] \tag{12}$$

where τ is the fatigue life of materials at load; σ is the applied pretension; T is the absolute temperature; τ_0 is the period of thermal fluctuations of atoms; U_0 is the energy of the rupture of an interatomic bond; α is the coefficient of overstress in the bond being ruptured; K is Boltzmann constant. We can obtain equation (13) from equation (12)

$$\ln N = A - \mathrm{B}\sigma \tag{13}$$

where $A = \ln \tau_0 + U_0/KT - \ln(2\pi/\omega)$; $B = \alpha/KT$

The $S-N$ curve of the single Kevlar 49 fiber at different bending angles is shown in Fig. 8 (a). It can be seen that the bending fatigue life of the Kevlar 49 fiber is decreased with the increase of pretension when the bending angle remains the same. The fatigue life of Kevlar 49 fiber is longer at the small bending angle and pretension. It can be seen from Equation (13) that the process of the fiber fatigue is a gradually decreasing binding energy U_0 period. The fatigue life decreases with the increasing pretension. This is due to the increase of dissipative binding energy U_0 resulting from the increasing pre-tension at one time under the same bending angle. It also indicates that the Kevlar 49 fiber can be easily ruptured at a large bending angle. The main reason is that the binding energy dissipation energy U_0 increases with the increase of bending angle. The fatigue life decreases with the increasing bending angle when the pretension remains the same. It also proves that the effects of large pretension with small bending angle and small pretension with large bending angle on the fatigue lifetime are the same.

The S-lnN curve is shown in Fig. 8 (b), where the y-axis is the logarithmic values of cyclic numbers. According to the data analysis, the linear relationship between the pretension σ and the

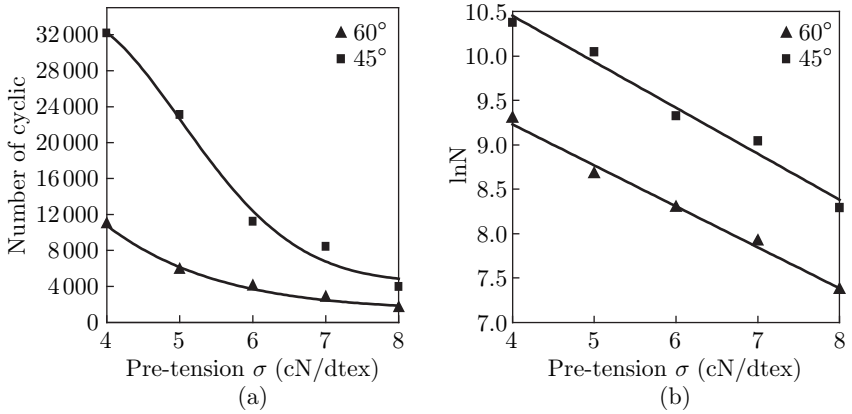

Fig. 8: (a) is the S-N curve of Kevlar 49 fiber; (b) is S-lnN curve of Kevlar 49 fiber

logarithmic values of fatigue numbers N can be obtained. Equation (14) shows the linear regression equations of the bending fatigue measurement and the corresponding correlation coefficient r at different bending angles θ (60°, 45°) respectively

$$\begin{aligned} \ln N &= 11.08 - 0.46\sigma, \quad r^2 = 0.988 \\ \ln N &= 12.53 - 0.52\sigma, \quad r^2 = 0.973 \end{aligned} \tag{14}$$

It can be found that there is a linear relationship between the pretension and the logarithmic value of bending fatigue life, in which the correlation coefficient r is relatively high. These results are consistent with Equation (13).

3.4 The Fracture Ends Morphology of Kevlar 49 Fiber

Fig. 9 (a) to 9 (c) show the fatigue failure ends morphology of Kevlar 49 fiber. From these morphologies we can see that the Kevlar 49 fiber are broken due to the fibrillation or axial split and the fracture ends morphology as "brush" and the bending fatigue rupture of Kevlar 49 fiber is typical fibrils splitting. The main reason is that the fiber is repeatedly stretched and compressed in the process of repeated bending, which leads to the decrease of the force between the fiber macromolecule.

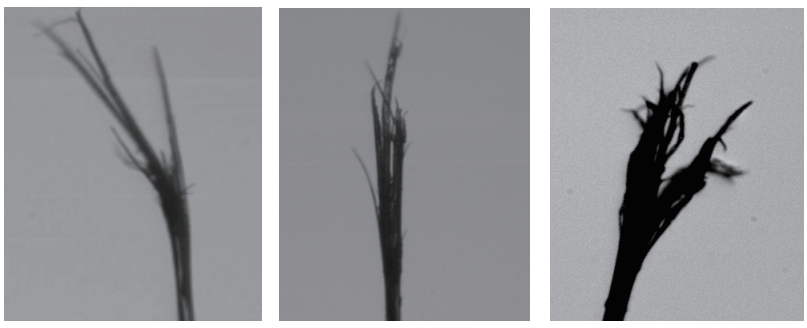

Fig. 9: Fracture end morphology of Kevlar 49 fiber

3.5 Discussion on the Fracture Mechanisms of the Bending Fatigue of Kevlar 49 Fiber

It is evident that the reason for the breakage of Kevlar 49 due to the fibrillation or long axial split, which can be explained by the fibrillar structure, the high orientation and low intermolecular force. Many previously study discussed on the bending fatigue fracture morphology of fibes. Scarcely study report on the character of bending fatigue fracture process of fiber. The Fig. 10 (a) – 10 (d) show morphologies of the Kevlar 49 fiber during the bending fatigue process, which are in-suit observed by microscope in experiment. The pre-tension is 8 cN/dtex and the bending angel is 45° in experiment. Fig. 10 (a) shows the morphology of the fiber before bending. In Fig. 10 (b), the fiber has suffered the extensive surface abrasion, fibrils occur and rupture near the bending point at its outer layer. But the fibril breakage only happened on one side. In Fig. 10 (c), assembled fibril flakes continue to rupture on two sides and some fibrils begin to fall off. In Figs. 10 (d) and 10 (e), fibrils further rupture near the bending point, then many fibrils rupture, severe splitting occurs on the fiber surface, so the diameter of fiber becomes finer. When the fiber was bent, the first separation occurred fibrillation, followed by individual or fibrillation bundles have broken until a serious split fibrillation.

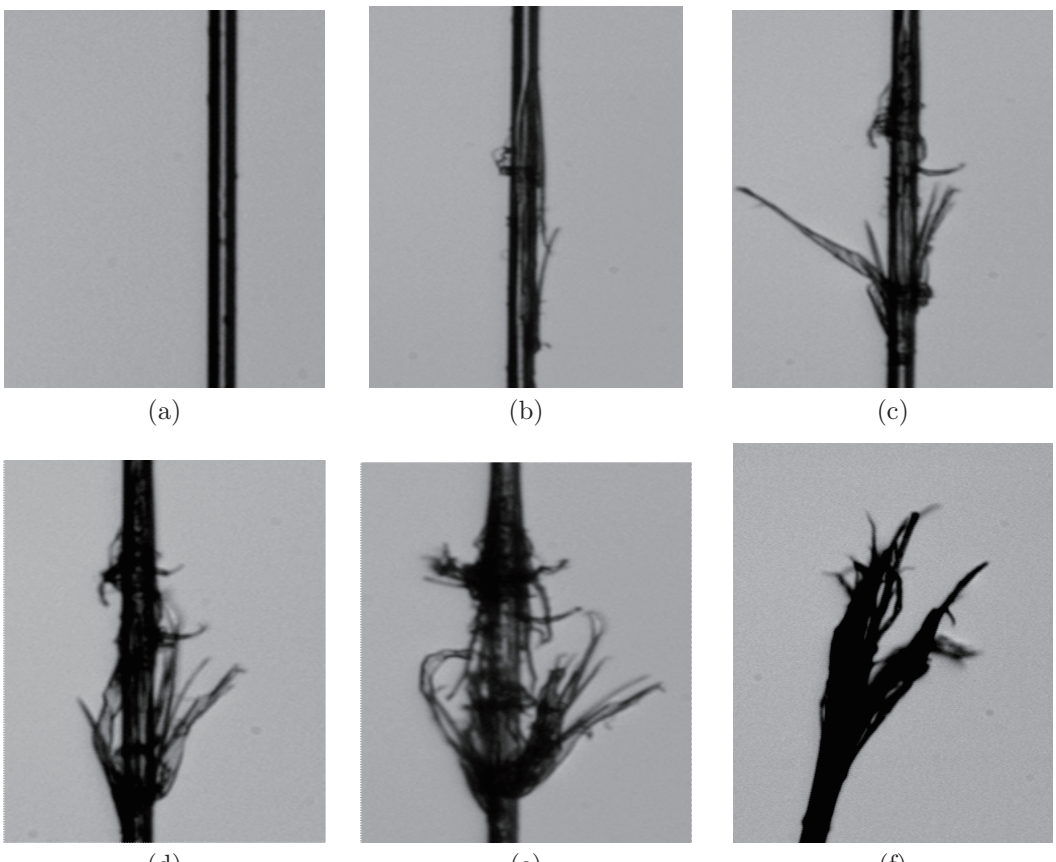

Fig. 10: The fracture morphologies of Kevlar 49 fiber under bending fatigue processing; (a) Before bending; (b) 300 cycles under 8 cN/dtex pretension; (c) 600 cycles under 8 cN/dtex pretension; (d) and (e) are 900 cycles and 1200 cycles under 8 cN/dtex pretension respectively; (f) The fracture end

4 Conclusion

In this paper, a novel bending fatigue test method is introduced and is used to study the bending fatigue behavior of single Kevlar 49 fiber. The apparatus can record the cyclic tension and has an optical system which can be used to in-situ observe and record the bending fatigue fracture process and cyclic bending fatigue number. The bending fatigue behavior of the Kevlar 49 fiber was discussed based on the S-N and S-lnN curve. It was found that the Kevlar 49 fiber can be easily ruptured at a large bending angle and pretension. There is a linear relationship between the pretension, bending angle and the logarithmic value of fatigue lifetime. Morphologies of Kevlar 49 fiber under the bending fatigue process, show that the fracture end of the Kevlar 49 fiber takes on the "brush".

References

[1] Hearle, JWS. High Performance Fibers [M]. WoodheadPub, 2011: 1-2.

[2] Christophe LC, Monasse B and Bunsell AR. Influence of temperature on fracture initiation in PET and PA66 fibres under cyclic loading [J]. Journal of Materials Science. 2007; 42: 9276-9283.

[3] Davies P and Bunsell AR. Tensile fatigue behaviour of PBO fibres [J]. Journal of Materials Science. 2010; 45: 6395-6400.

[4] Herrera JM, Ramirez AR and Bunsell AR. Microstructural mechanisms governing the fatigue failure of polyamide 66 fibres [J]. Journal of materials science. 2006; 41: 7261-7271.

[5] Konopasek L and Hearle JWS. The tensile fatigue behavior of aramid fibers and their fracture morphology [J]. Journal of Applied Polymer Science 1997; 21: 2791-2815.

[6] Hearle JWS. Fatigue failure of textile fibres [M]. WoodheadPub, 2011: 34-52.

[7] Liu XY, Yu WD. Bending fatigue properties of single aramid fibers. In: Chemical Fibers International 2004; 54: 173.

[8] C.J.Burgoyne, R.E. Hobbs and J. Strzemiecki, 8th Int Conf on Offshore Mechanics and Arctic Engineering, pp.691-698, The Hague, 1989.

[9] Kazuto T, Kohji M, Takahiro O and Kenjiro K.Influences of stress waveform and wet environment on fatigue fracture behavior of aramid single fiber [J]. Composites Science and Technology. 2004; 64: 1531-1537.

[10] Kohji M,Yoshihiro M and Kenjiro K. The influence of vacuum on fracture and fatigue behavior in a single aramid fiber [J]. International Journal of Fatigue. 2000; 22: 757-765.

[11] Cai GM, Wang XG, Shi XJ and Yu WD. Evaluation of fatigue properties of high performance fibers based on fixed-point bending fatigue test [J]. Journal of Composite Materials. 2012; 7: 831-840.

[12] Cai GM, Yu WD. Characterization for bending fatigue properties of PBO fiber [J]. Industria Textila. 2010; 4: 163-167.

[13] Yu WD, Du ZQ and Cai GM. A microscale positioning device of single fiber bending fatigue: China patent No.10304650, 2011.